

Electronic Properties in a Five-Coordinate Azido Complex of Nonplanar Iron(III) Porphyrin: Revisiting to Quantum Mechanical Spin Admixing

Saburo Neya,*[1] Akihiro Takahashi,[1] Hirotaka Ode,[1] Tyuji Hoshino,[1] Akira Ikezaki,[2] Yoshiki Ohgo,[2] Masashi Takahashi,[3] Yuji Furutani,[4] Víctor A. Lórenz-Fonfría,[4] Hideki Kandori,[4] Hirotsugu Hiramatsu,[5] Teizo Kitagawa,[5] Junji Teraoka,[6] Noriaki Funasaki,[7] and Mikio Nakamura[2]

[1]Department of Physical Chemistry, Graduate School of Pharmaceutical Sciences, Chiba University, Yayoi-cho, Inage-ku, Chiba 263-8522

[2]Department of Chemistry, School of Medicine, Toho University, Omorinishi, Ota-ku, Tokyo 143-8540

[3]Department of Chemistry, Faculty of Science, Toho University, Funabashi 274-8510

[4]Department of Material Science and Engineering, Nagoya Institute of Technology, Nagoya 466-8555

[5]Center for Integrative Bioscience, Okazaki National Institutes, Okazaki 444-8787

[6]Graduate School of Science, Osaka City University, Sugimoto, Osaka 558-8585

[7]Department of Physical Chemistry, Kyoto Pharmaceutical University, Yamashina, Kyoto 607-8414

Received August 7, 2007; E-mail: sneya@p.chiba-u.ac.jp

The iron(III) azido complex of 5,10,15,20-tetraisopropylporphyrin was characterized with NMR, EPR, Mössbauer, and magnetic susceptibility. These physical methods indicate mixing of the high ($S = 5/2$) and intermediate ($S = 3/2$) spin-states of the iron atom. The results were interpreted in terms of the core contraction after nonplanar deformation of porphyrin ring by the bulky isopropyl substituents. In the IR spectrum of this complex, there are two signals at 2062 and 2048 cm^{-1} due to the antisymmetric vibration of the coordinated azido ligand. The split IR bands demonstrate that the two spin isomers are present, and that the $S = 5/2$ and $3/2$ transition occurs sufficiently slow on the IR timescale. This is in remarkable contrast with the homogeneous spin-mixing model proposed for the $S = 5/2$ and $3/2$ system. The present observations further suggests that the three $S = 5/2$, $3/2$, and $1/2$ states in iron(III) porphyrin commonly mix through thermal spin equilibrium.

Porphyrin is a biological pigment found in hemoprotein as the prosthetic group. The relation between porphyrin structure and biological activity of the protein has been the subject of continuing interest. The flat macrocycle is not necessarily rigid and tends to deviate from planarity by structural perturbations. The heme in protein, for example, is nonplanar due to steric constraints in the crowded protein pocket.[1] The porphyrin-placed outside protein pocket could be still deformed if bulky substituents are peripherally attached. The enforced deformation by large-sized substituents is typically found in dodeca-substituted porphyrins and 5,10,15,20-(*tert*-butyl)porphyrins.[2]

Distortion in porphyrin macrocycle contracts the coordination core to affect the electronic state of the iron atom. Ikezaki and Nakamura have reorted that the common $(d_{xy})^2(d_{xz}, d_{yz})^3$ configuration of iron(III) changes into the less common $(d_{xy})^1(d_{xz}, d_{yz})^4$ configuration in a ruffled heme.[3] They have further found a novel type of equilibrium between the low-spin ($S = 1/2$) and intermediate-spin ($S = 3/2$) states for a saddled heme.[4,5] Another interesting observation in nonplanar iron(III) porphyrin is the coexistence of the intermediate- ($S = 3/2$) and high-spin ($S = 5/2$) states. The mixing of the $S = 5/2$ and $3/2$ states in ordinary iron porphyrin is induced only by bulky and weak axial-ligands, such as ClO_4^- and $C(CN)_3^-$,[6–8] and the small chloride ligand brings about the high-spin state. However, the spin-mixing occurs with a chloride ligand when the heme plane is nonplanar.[9,10]

The $S = 3/2$ state of hemoprotein is found in cytochrome c' and horseradish peroxidase.[11,12] Maltempo and Moss have proposed a theoretical model, in which the $S = 5/2$ and $3/2$ states couple through spin–orbit interaction to create a new and discrete ground-state in these hemoproteins.[13] Quantum mechanical spin-coupling is different from spin crossover in that the resultant state is homogeneous in the former, whereas it is heterogeneous in the latter. The Maltempo model has been frequently postulated for the iron(III) porphyrins in the mixed $S = 5/2$ and $3/2$ state.[6,7] Ohgo et al. have recently shown for a saddled iron(III) porphyrin that the $S = 5/2$ and $3/2$ states are in thermal equilibrium below 5 K.[14] We have recently demonstrated another example of the $S = 5/2$ and $3/2$ equilibrium for iron(III) azido complex of porphycene, a porphyrin isomer.[15] In the porphycene, the $S = 5/2$ and $3/2$ equilibrium is observed over a wide temperature range below 300 K. These results are in remarkable contrast with the Maltempo model.[13] However, this may be limited to porphycene[15] and a highly deformed heme at extremely low temperatures.[14] One could argue that quantum mechanical spin-couling[13] still holds true for other porphyrins. Accordingly, the further understanding of spin admixing process is necessary for iron porphyrins.

Published on the web January 10, 2008; doi:10.1246/bcsj.81.136

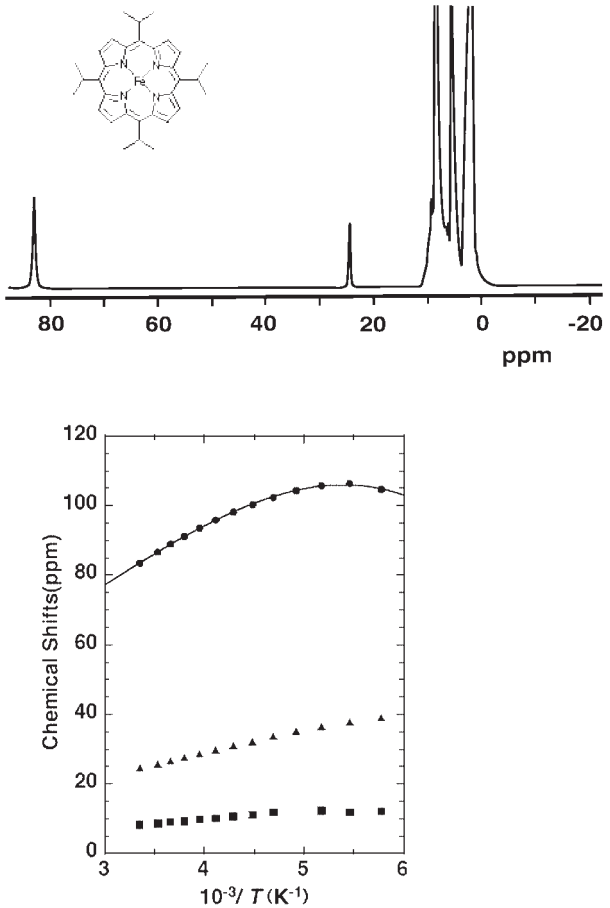

Fig. 1. (Upper) Proton NMR spectrum of [FeN_3(tiprp)], (inset) in CD_2Cl_2 at 298 K. (Lower) Temperature dependence of the NMR shifts. The solid curve for the pyrrole-H shift (●) is the theoretical fit calculated with the parameters in the text. The shifts for the CH and CH_3 protons are indicated with ▲ and ■, respectively.

The main focus the present work is exploration of the mechanism by which the spin states are admixed. We studied (5,10,15,20-tetraisopropylporphyrinato)iron(III), [Fe(tiprp)][16,17] (Fig. 1, inset), because the compound has close structural relevance to other nonplanar porphyrins where the $S = 5/2$ and $3/2$ mixing has been evoked.[7,10] We present here detailed characterization of the azido derivative [FeN_3(tiprp)]. Although the results contain contradictory results between the magnetic and vibrational measurements, elucidation on the timescale of the physical methods consistently showed that the $S = 5/2$ and $3/2$ states in iron(III) porphyrins are in thermal equilibrium.

Materials and Methods

Tiprp and [FeN_3(tiprp)]. 5,10,15,20-Tetraisopropylporphyrin [H_2(tiprp)] was prepared by using the following procedure. Pyrrole (4.2 mL) and isobutyraldehyde (5.6 mL) were added to propionic acid (300 mL) containing water (6 mL) at 100 °C in beaker covered with a glass plate. The solution was stirred at 100 °C over 2 h and cooled to room temperature before addition of chloroform (450 mL). The mixture was washed with dilute aqueous sodium hydroxide (0.1 M, 450 mL × 2) and water (450 mL × 2) to remove propionic acid. Chloranil (4.5 g) was added to the chloroform solution, and the solution was stirred at 60 °C for 30 min. Methanol (150 mL) was added to the cooled chloroform and air was bubbled into the solution for 1 h. The organic mixture was evaporated to dryness, and the residue was washed on a centrifuge with small portions of methanol (10 mL × 10) to eliminate tar. The crude porphyrin was purified on a silica-gel column with chloroform, and the solvent was evaporated to dryness. Thin-layer chromatography at this stage showed two porphyrin-like bands. The residue was then further purified on a silica-gel column to separate off an unidentified by-product. Elution with chloroform–acetic acid (10:1, v/v) removed the by-product. The main product was then eluted as the second band with chloroform–pyridine (20:1, v/v), washed with water, and the solvent was evaporated to dryness. The porphyrin was then crystallized from chloroform–methanol (1:1, v/v). Yield 396 mg (5.4% yield). Anal. Calcd for $C_{32}H_{38}N_4$: C, 80.29; H, 8.00; N, 11.71%. Found: C, 79.86; H, 8.12; N, 11.90%. MS: m/z 478. ^{1}H NMR (400 MHz, $CDCl_3$, δ): 9.50 (s, 8H, pyrrole-H), 5.36 (sept, 4H, α-CH), 2.36 (d, 24H, β-CH_3), −1.73 (br s, 2H, NH).

A dimethylformamide solution (20 mL) containing tiprp (100 mg) and $FeCl_2 \cdot 4H_2O$ (300 mg) was heated at 85 °C for 30 min under nitrogen to afford the iron complex. The cooled solution was bubbled with air to oxidize the iron, mixed with chloroform (50 mL), washed with brine (50 mL × 4, pH 5 with HCl), and evaporated to dryness. The crude [FeCl(tiprp)] was passed through a silica-gel column with chloroform–methanol (20:1, v/v). The purified [FeCl(tiprp)] was dissolved in benzene, vigorously mixed overnight with 5 M aqueous NaN_3[18] to afford [FeN_3(tiprp)]. Formation of [FeN_3(tiprp)] was confirmed with the ^{1}H NMR spectrum, in which the hyperfine-shifted peaks of [FeCl(tiprp)] were replaced with those of [FeN_3(tiprp)]. [FeN_3(tiprp)] was recrystallized from benzene. Anal. Calcd for $C_{32}H_{36}FeN_7$: C, 66.90; H, 6.32; N, 17.07%. Found: C, 67.20; H, 6.67; N, 17.36%. MS: m/z 574.

Physical Measurements. ^{1}H NMR spectra at 300 MHz were recorded on a JEOL LA300 with a temperature variation unit, and chemical shifts were referenced to the residual peak of CD_2Cl_2 at 5.32 ppm. The X-band EPR spectra were recorded on a Bruker E500 spectrometer equipped with an Oxford helium cryostat. IR spectra were obtained on a Digilab FTS-7000 spectrometer equipped with an Oxford cooling unit.[19] The IR curve-fitting was carried out after Lórenz-Fonfría and Padrós.[20] ^{57}Fe Mössbauer spectra were measured on a Wissel Mössbauer spectrometer system. The sample was kept in a gas-flow cryostat and ^{57}Co(Rh) source was kept at room temperature. Isomer shifts δ_{Fe} was referenced to α-iron at room temperature. Solid-state magnetic susceptibilities were measured over a temperature range of 5–300 K at 1 T on a Quantum Design MPMS-7 SQUID magnetometer. The data were corrected for both the diamagnetism of the basket and molecule Pascal's constants.

Results

^{1}H NMR, EPR, and Mössbauer. We monitored the magnetic properties of [FeN_3(tiprp)] with ^{1}H NMR. Figure 1 shows the NMR spectrum at 298 K where a set of pyrrole-H (=2, 3, 7, 8, 12, 13, 17, 18H), α-CH (=5^1, 10^1, 15^1, 20^1H), and β-CH_3 (=5^2, 10^2, 15^2, 20^2H) signals were observed at 83.4, 24.6, and 8.2 ppm, respectively. The assignment is based on the NMR results of a related compound [FeCl(tiprp)].[16] The pyrrole-H shift of 83.4 ppm is consistent with a 5-coordinate high-spin iron(III) complex.[21] However, the pyrrole-H signal did not follow the Curie law, and the $1/T$ dependence

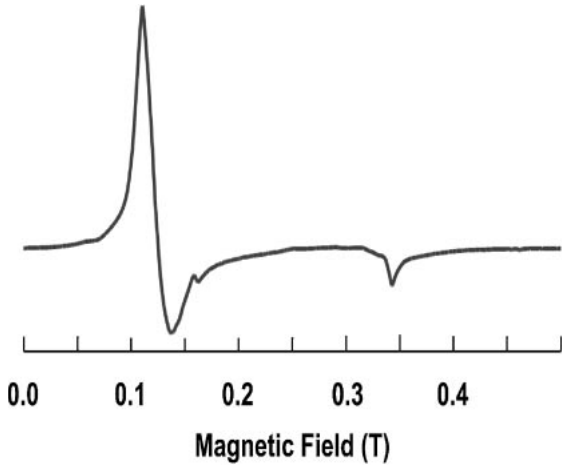

Fig. 2. EPR spectrum of frozen dichloromethane solution of [FeN_3(tiprp)] with $g = 5.44$ and 1.99 at 5 K.

was nonlinear. Similar NMR results have been reported for Fe(tiprp)X (X = Br and I),[22] for which the Curie plots are also markedly nonlinear. The similarity likely comes from the close ligand-field splitting parameters among N_3^-, Br^-, and I^- ions.[23] The unusual NMR behavior in Fig. 1 suggests that [FeN_3(tiprp)] is not in a pure high-spin state.

Figure 2 displays the EPR spectrum of [FeN_3(tiprp)] recorded at 5 K. The spectrum shows nearly axial symmetric spectrum with $g_\perp = 5.44$ and $g_\parallel = 1.99$ signals. The $g_\perp$ value is between those of the typical high-spin ($g_\perp = 6$) and intermediate-spin ($g_\perp = 4$) species. Another notable observation is the significant temperature dependence; the EPR spectrum broadened out above 10 K and provided no observable signals at 77 K. This is in contrast with ordinary iron(III) high-spin heme complexes that exhibit clear high-spin EPR signals at 77 K.[24]

We recorded Mössbauer spectra to further examine the anomalies as inferred from the NMR and EPR. In Fig. 3 are shown the Mössbauer spectra of powder [FeN_3(tiprp)] at 290 K. The isomer shift was $\delta_{Fe} = 0.31\,mm\,s^{-1}$ and quadrupole splitting was $\Delta E_q = 1.00\,mm\,s^{-1}$. The ΔE_q is intermediate between 0.8 and 3.2, which are typical value for the $S = 5/2$ and $S = 3/2$ states, respectively.[25] The Mössbauer parameters were temperature dependent, and gradually changed to $\delta_{Fe} = 0.39\,mm\,s^{-1}$ and $\Delta E_q = 1.07\,mm\,s^{-1}$ at 77 K.

Magnetic Susceptibility. Magnetic moment provides the direct and quantitative evaluation of the metal center. Figure 4 shows the magnetic susceptibility of microcrystalline [FeN_3(tiprp)] recorded over a temperature range of 5–300 K. The effective magnetic moment was $5.43\,\mu_B$ at 290 K and gradually decreased to $5.05\,\mu_B$ at 50 K. The values are intermediate between 5.92 and $3.87\,\mu_B$ of the pure $S = 5/2$ and 3/2 states, respectively.

Analysis of Isotropic Shifts. The unusual pyrrole-H shift for [FeN_3(tiprp)] in Fig. 1 was quantitatively analyzed on the basis of a two-state model. The observed isotropic shift δ consists of diamagnetic and isotropic contributions.[21] A pyrrole-H shift of 9.5-ppm, estimated from the free base spectrum, was employed as the diamagnetic reference. Thus, we obtained $\delta - 9.5 = \alpha\delta_I + (1-\alpha)\delta_{II}$, where $\delta_I = A/T$ and $\delta_{II} = B/T$ are the isotropic shifts of the states I and II, respectively. Constants A and B define the slope of straight lines in the Curie

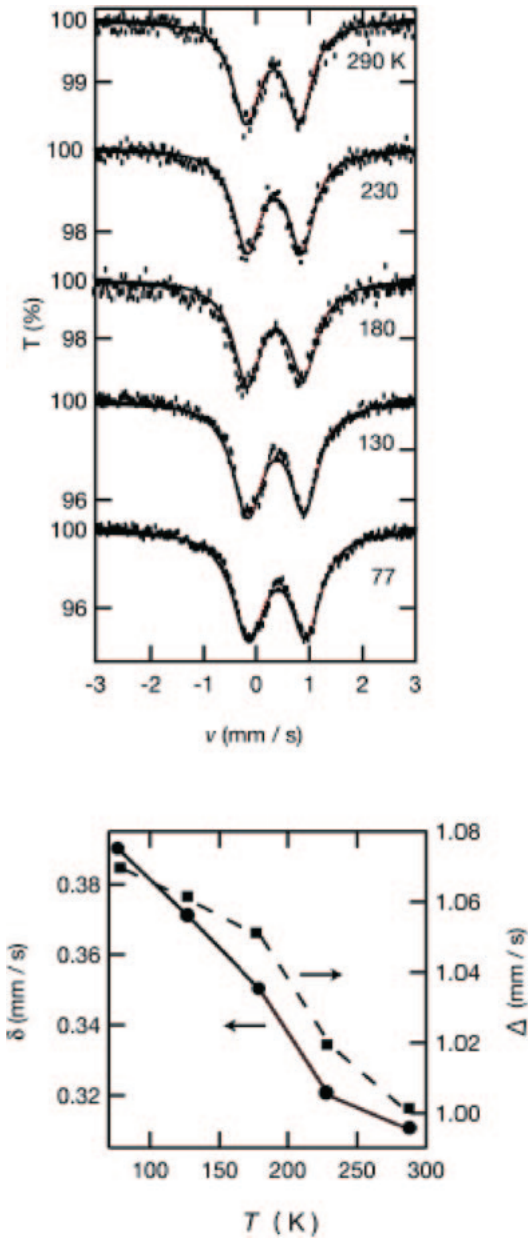

Fig. 3. (Upper) Solid-state Mössbauer spectra of [FeN_3-(tiprp)]. (Lower) Temperature dependence of quadrupole splitting ΔE_q and isomer shift δ_{Fe}.

plots, and α and $(1-\alpha)$ represent the fractions of the I and II components. The isotropic shift is subsequently expressed as $\delta - 9.5 = \alpha(A/T) + (1-\alpha)(B/T)$, and the equilibrium constant is formulated as $K = [I]/[II] = \alpha/(1-\alpha) = [A - T(\delta - 9.5)]/[T(\delta - 9.5) - B]$. We can write the van't Hoff equation $\ln K = -\Delta H/RT + \Delta S/R$ as

$$\ln\frac{A - T(\delta - 9.5)}{T(\delta - 9.5) - B} = \frac{\Delta H}{R}\frac{1}{T} - \frac{\Delta S}{R}. \quad (1)$$

The observed pyrrole-H shifts δ in Fig. 1 were analyzed with the van't Hoff formalism. Parameters A and B were varied at 10 ppm K intervals in a $(A, B) = (50000$ to $20000, -5000$ to $-30000)$ region to look for an (A, B) set that gives rise to the best linear correlation. We employed for this analysis the computer program that was used to analyze the thermo-

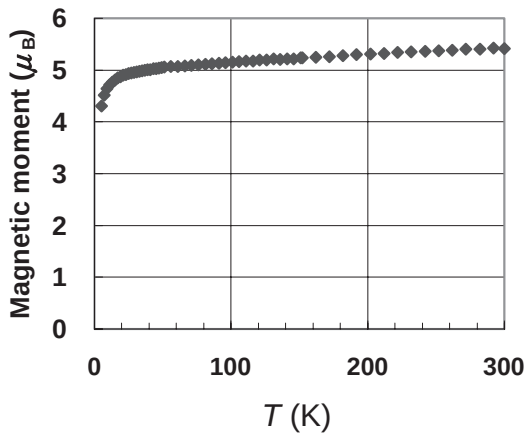

Fig. 4. Temperature dependence of the effective magnetic moments of microcrystalline [FeN_3(tiprp)].

chromism and isotropic shifts in hemoproteins.[26,27] The best linear correlation was obtained at (A, B) = (23870, −15800) with a correlation coefficient 0.99984, corresponding to $\Delta H = -1280\,\mathrm{cal\,mol^{-1}}$ and $\Delta S = -10.3\,\mathrm{cal\,mol^{-1}\,K^{-1}}$. The solid curve for the pyrrole-H signal in Fig. 1 represents the theoretical fit calculated with these parameters. We obtained an equilibrium constant of $K = [\mathrm{I}]/[\mathrm{II}] = \Delta H/\Delta S = 19.0$ at 295 K.

IR Spectra. IR spectroscopy, when applied to the iron-bound ligand, provides a sensitive probe for the reaction center of metalloproteins.[18,27] Figure 5 shows the azide stretching region in the IR spectra of [FeN_3(tiprp)] with three absorption bands at 2108, 2062, and 2023 $\mathrm{cm^{-1}}$. The former two bands are asymmetric, and peak analysis resolved five symmetric bands at 2112, 2102, 2068, 2062, and 2048 $\mathrm{cm^{-1}}$. We assigned, from the IR similarity with [FeN_3(porphycene)],[15] the two peaks at 2062 and 2048 $\mathrm{cm^{-1}}$ to the antisymmetric stretching mode of the coordinating azide, and the other bands to vibrational bands from the porphyrin. The integrated intensity ratio of the two bands was $I_{2048}/I_{2062} = 6/94$ at 293 K. The ratio was temperature dependent and changed from 8/92 at 254 K to 13/87 at 216 K. Other peak intensities were virtually temperature independent.

Discussion

Mixing of the $S = 3/2$ State. The iron(III) azido complexes of ordinary porphyrin are known to be pure high-spin.[15,18,28] In contrast, [FeN_3(tiprp)] is not pure high-spin: the hyperfine-shifted pyrrole-H NMR chemical shift does not follow the Curie law (Fig. 1), and the EPR (Fig. 2) and Mössbauer parameters (Fig. 3) are intermediate between those of typical $S = 5/2$ and $S = 3/2$ compounds. The magnetic susceptibility of 5.43 μ_B at room temperature (Fig. 4) is also intermediate between the spin-only values for the high- and intermediate-spin states These results suggest that [FeN_3(tiprp)] has a mixed $S = 5/2$ and 3/2 character. Lowering the temperature shifts the $S = 5/2$ and 3/2 equilibrium toward the $S = 3/2$ state as evidenced by the magnetic susceptibility and Mössbauer results. States I and II assumed in the above NMR analysis were thus assigned to be the $S = 3/2$ and 5/2 isomers, respectively.

The $S = 3/2$ character in [FeN_3(tiprp)] likely comes from

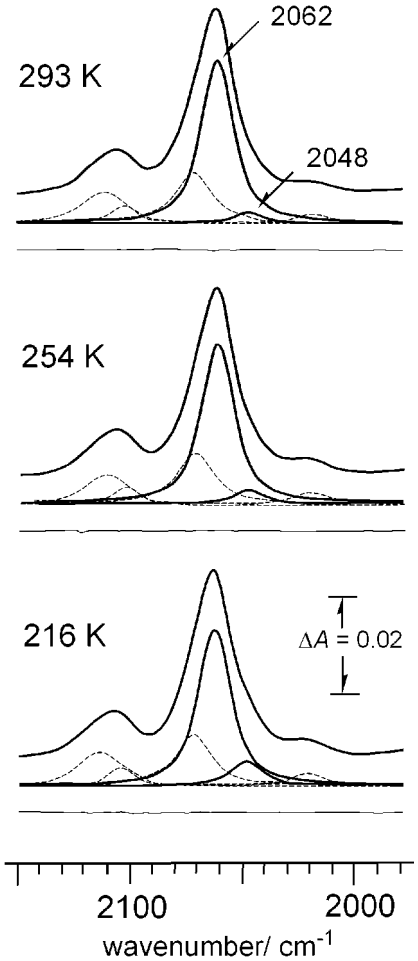

Fig. 5. Temperature-dependent IR absorption of the iron-bound azido of [FeN_3(tiprp)]. The resolved curves and residuals are indicated. Sample concentration is about 1 mM in chloroform.

deformation of the porphyrin core. From the crystallographic analysis, the iron complex is not planar due to steric repulsion from the bulky isopropyl groups, and the coordination core is somewhat contracted to shorten the iron–pyrrole bonds.[16] Equatorial ligand-field of the iron(III) atom is accordingly strengthened, and the axial iron–ligand is weakened on the nonplanar deformation. Partial $S = 3/2$ character in nonplanar [FeN_3(tiprp)] is also probable, because the ligand-field splitting parameters of Br^-, I^-, and N_3^- are similar to each other[23] and because the [FeX(tiprp)] (X = Br and I) complexes exhibit partial $S = 3/2$ character.[22]

Azido Stretching Bands. The important IR result of [FeN_3(tiprp)] is the split bands of the coordinating azido ligand (Fig. 5). The result is in contrast with a single azido band in ordinary iron porphyrin.[15,18,28] For the split IR bands, there are several possible explanations, such as sample contamination by free azido, solvent contamination by water, occurrence of the bis-azido species, rotation of the coordinating azide about the axial bond, and Fermi resonance. However, these possibilities are excluded as we have already discussed in the [FeN_3(porphycene)] case.[15] We assigned the 2062 and 2048 $\mathrm{cm^{-1}}$ peaks to the $S = 5/2$ and 3/2 isomers, respectively. The assignment is based on the results that [FeN_3-

(porphycene)] exhibits the two azide bands at 2066 ($S = 5/2$ state) and 2049 cm^{-1} ($S = 3/2$ state),[15] and that the peak position is insensitive to the molecular shape of the porphyrinoids.[29] The two IR bands in [FeN_3(tiprp)] are consistent with the two spin isomers on the basis of NMR, EPR, Mössbauer, and magnetic susceptibility. It should be noted that the 2048 cm^{-1} peak assigned to the $S = 3/2$ species increased at lower temperatures: $I_{2048}/I_{2062} = 6/94$ (293 K), 8/92 (254 K), and 13/87 (216 K). Since the azido peak intensities in IR spectrum reflect the population of the spin isomers,[15,18,26,29] the intensity ratios directly correlate to the equilibrium constants of $[S = 3/2]/[S = 5/2]$. The values obtained with IR are in good agreement with the $[S = 3/2]/[S = 5/2]$ ratios, 5/95 (293 K), 7/93 (254 K), and 9/91 (216 K), calculated from the thermodynamic parameters obtained from NMR analysis (Fig. 1). Consistency between the IR and NMR results supports the validity of the physical analyses.

Homogeneous or Heterogeneous? It has been proposed that the $S = 5/2$ and $S = 3/2$ states couple quantum mechanically through spin–orbit interactions to create a new discrete ground state. The resultant mixture is assumed to be magnetically homogeneous.[13] The primary support for the assumption comes from Mössbauer and EPR, which exhibited a single set of signals.[7] These physical methods conventionally are good enough to resolve the distinct spin isomers in the iron(III) and iron(II) complexes.[30,31] For the iron(III) porphyrins with mixed $S = 5/2$ and $3/2$ character, only one set of signals has been detected,[6,7] and the result is consistent with the spin-admixing model by Maltempo.[7,12] For [FeN_3(tiprp)], the Mössbauer and EPR provide single sets of signals. However, there were two signals of the iron-bound azido, as seen in Fig. 5. The two IR bands demonstrate that the distinct $S = 5/2$ and $S = 3/2$ isomers undergo sufficiently slow interconversion on the IR timescale and that the two states are heterogeneously admixed. The contradiction between IR and EPR/Mössbauer is resolved by realizing the temporal resolution of applied physical methods. The typical frequencies of Mössbauer, EPR, and IR are approximately 10^7, 10^{10}, and 10^{13} s^{-1}, respectively.[32,33] Excellent time resolution of IR over Mössbauer and EPR could resolve the rapid exchanging processes. We could estimate the minimum life time of the two species to be $\tau = 0.4$ ps from the relationship $\tau = 1/(2\pi\Delta\nu)$[34] where $\Delta\nu$ = (light velocity) × (IR peak separation) (Fig. 5). The exchange rate of the spin isomers is thus roughly fixed in the range of 10^{11}–10^{12} s^{-1} from the EPR and IR results. The $S = 5/2$ and $3/2$ exchange rate in [FeN_3(tiprp)] is much larger than that measured for the $S = 5/2$ and $1/2$ transition (4×10^7 s^{-1}) in the hydroxide complex of myoglobin.[35]

Comparison with Porphycene. It is notable that the population of the $S = 3/2$ isomer for [FeN_3(tiprp)] is only 0.05 at room temperature whereas it is 0.24 for [FeN_3(porphycene)].[15] The larger $S = 3/2$ character in [FeN_3(porphycene)] is reflected as a clear shoulder band in the IR spectrum, upfield-shifted pyrrole-H NMR signal, and EPR value close to $g_\perp = 4.0$.[15] A larger $S = 3/2$ population in the porphycene complex arises from the characteristic structure of the coordination cavity. Porphycene has a narrower metallo core than tiprp, and the Fe–N(pyrrole) bond is shorter in [FeCl(porphycene)] (1.96 Å)[36] than that in [FeCl(tiprp)] (2.04 Å).[16] A longer Fe–pyrrole bond is reasonably expected for the azido complexes as well. The longer equatorial bonds of [FeN_3(tiprp)], as compared with [FeN_3(porphycene)], in turn causes a shorter axial Fe–azido bond. These structural perturbations stabilize the $d_{x^2-y^2}$ orbital and destabilize the iron d_{z^2} orbital to cause the smaller intermediate-spin character in [FeN_3(tiprp)] than in [FeN_3(porphycene)]. Accordingly, the larger metallo hole causes the lower midpoint in the spin transition calculated from $\Delta H/\Delta S$. [FeN_3(tiprp)] ($T_{1/2} = 124$ K) exhibits a lower transition temperature than [FeN_3(porphycene)] ($T_{1/2} = 242$ K).[15]

Mechanistic Implications. The above observations indicate that [FeN_3(tiprp)] is in an equilibrium between the $S = 5/2$ and $3/2$ states, suggesting that the occurrence of spin-crossover phenomenon is not special to the two iron(III) chelates of saddled porphyrin and porphycene.[14,15] A mixed $S = 5/2$ and $3/2$ state has also been reported for [FeX(tiprp)][15] and [FeX(porphycene)] (X = Br or I).[37] In these compounds, however, it is unclear whether the quantum mechanical spin-admixing or spin-crossover occurs. The present results suggest that [FeX(tiprp)]s[16] (X = Br and I) are the $S = 5/2$ and $3/2$ equilibrium systems. The heterogeneous mixing of the $S = 5/2$ and $S = 3/2$ states is in marked contrast with the homogeneous spin-admixing model.[13]

Iron(III) porphyrin can adopt three spin states, and thus three different equilibria are possible. The $S = 5/2$ and $1/2$ equilibrium in many hemes and hemoproteins has been intensively characterized.[18,26,27,29] Another equilibrium between the $S = 3/2$ and $1/2$ states has recently been observed in both heme and heme oxygenase.[4,5,38] On the other hand, the spin equilibrium between the $S = 5/2$ and $S = 3/2$ systems has been so far ruled out.[7,12,17] Present IR result for [FeN_3(tiprp)] provides a novel picture that the $S = 5/2$ and $3/2$ states are in thermal equilibrium just as the $S = 5/2$, $1/2$ and $S = 3/2$, $1/2$ systems.[15] From these observations for the mixed-spin $S = 5/2$, $1/2$, $S = 3/2$, $1/2$, and $S = 5/2$, $3/2$ systems, we concluded that the spin mixing in iron(III) porphyrin complexes commonly proceed through thermal spin equilibrium.

We are grateful to the Research Center for Molecular-Scale Nanoscience and the Institute for Molecular Science for assistance in obtaining the EPR and magnetic moment. This work was supported by Grants-in-Aid from the Japanese Society for the Promotion of Science (# 18590094).

References

1 J. A. Shelnutt, X.-Z. Song, J.-G. Ma, S.-L. Jia, W. Jentzen, C. J. Medforth, *Chem. Soc. Rev.* **1998**, *27*, 31.

2 M. O. Senge, in *The Porphyrin Handbook*, ed. by K. K. Kadish, K. M. Smith, R. Guilard, Academic Press, New York, **2000**, Vol. 1, pp. 239–347.

3 A. Ikezaki, M. Nakamura, *Inorg. Chem.* **2002**, *41*, 2761.

4 T. Ikeue, Y. Ohgo, T. Yamaguchi, M. Takahashi, M. Takeda, M. Nakamura, *Angew. Chem., Int. Ed.* **2001**, *40*, 2617.

5 Y. Ohgo, T. Ikeue, M. Nakamura, *Inorg. Chem.* **2002**, *41*, 1698.

6 D. R. Evans, C. A. Reed, *J. Am. Chem. Soc.* **2000**, *122*, 4660.

7 G. P. Gupta, G. Lang, Y. J. Lee, W. R. Scheidt, K. Shelly,

C. A. Reed, *Inorg. Chem.* **1987**, *26*, 3022.
8 D. H. Dolphin, J. R. Sams, T. B. Tsin, *Inorg. Chem.* **1977**, *16*, 711.
9 R.-J. Cheng, P.-Y. Chen, P.-R. Gau, C.-C. Chen, S.-M. Peng, *J. Am. Chem. Soc.* **1997**, *119*, 2563.
10 V. Schünemann, M. Gerdan, A. X. Trautwein, N. Haoudi, D. Mandon, J. Fischer, R. Weiss, A. Tabard, R. Guilard, *Angew. Chem., Int. Ed.* **1999**, *38*, 3181.
11 T. Yoshimura, S. Suzuki, T. Kohzuma, H. Iwasaki, S. Shidara, *Biochim. Biophys. Acta* **1990**, *169*, 1235.
12 G. R. Schonbaum, *J. Biol. Chem.* **1973**, *248*, 502.
13 M. M. Maltempo, T. H. Moss, *Q. Rev. Biophys.* **1976**, *9*, 181.
14 Y. Ohgo, Y. Chiba, D. Hashizume, H. Uekusa, T. Ozeki, M. Nakamura, *Chem. Commun.* **2006**, 1935.
15 S. Neya, A. Takahashi, H. Ode, H. Hoshino, M. Hata, A. Ikezaki, Y. Ohgo, M. Takahashi, H. Hiramatsu, T. Kitagawa, Y. Furutani, H. Kandori, N. Funasaki, M. Nakamura, *Eur. J. Inorg. Chem.* **2007**, 3188.
16 T. Ikeue, Y. Ohgo, A. Uchida, M. Nakamura, H. Fujii, M. Yokoyama, *Inorg. Chem.* **1999**, *38*, 1276.
17 M. S. Somma, C. J. Medforth, N. Y. Nelson, M. M. Olmstead, R. G. Khoury, K. M. Smith, *Chem. Commun.* **1999**, 1221.
18 S. McCoy, W. S. Caughey, *Biochemistry* **1970**, *9*, 2387.
19 H. Kandori, Y. Furutani, K. Shimono, Y. Shichida, N. Kamo, *Biochemistry* **2001**, *40*, 15693.
20 V. A. Lórenz-Fonfría, E. Padrós, *Analyst* **2004**, *129*, 1243.
21 H. M. Goff, in *Iron Porphyrins*, ed. by A. B. P. Lever, H. B. Gray, Addison-Wesley, London, **1983**, Part I, pp. 237–281.
22 T. Sakai, Y. Ohgo, A. Hoshino, T. Ikeue, T. Saitoh, M. Takahashi, M. Nakamura, *Inorg. Chem.* **2004**, *43*, 5034.
23 E. König, *Coord. Chem. Rev.* **1968**, *3*, 471.
24 W. E. Blumberg, *Methods Enzymol.* **1981**, *76*, 312.
25 J. R. Sam, T. B. Tsin, in *The Porphyrins*, ed. by D. Dolphin, Academic Press, New York, **1979**, Vol. 4, pp. 425–478.
26 S. Neya, S. Hada, N. Funasaki, J. Umemura, T. Takenaka, *Biochim. Biophys. Acta* **1985**, *827*, 157.
27 S. Neya, N. Funasaki, *Biochemistry* **1986**, *25*, 1221.
28 S. Neya, I. Morishima, *J. Am. Chem. Soc.* **1982**, *104*, 5658.
29 S. Neya, C. K. Chang, D. Okuno, T. Hoshino, M. Hata, N. Funasaki, *Inorg. Chem.* **2005**, *44*, 1193.
30 R. H. Petty, E. V. Dose, M. F. Tweedle, L. J. Wilson, *Inorg. Chem.* **1978**, *17*, 1064.
31 E. König, G. Ritter, S. K. Kulshreshtha, *Inorg. Chem.* **1984**, *23*, 1144.
32 R. J. Butcher, J. R. Ferraro, E. Sinn, *Inorg. Chem.* **1976**, *15*, 2077.
33 M. D. Timken, D. N. Hendrickson, E. Sinn, *Inorg. Chem.* **1985**, *24*, 3947.
34 D. F. Schreiver, P. W. Atkins, C. H. Langford, *Inorganic Chemistry*, 2nd ed., Oxford University Press, Oxford, **1994**, p. 113.
35 E. V. Dose, M. F. Tweedle, D. H. Turner, L. J. Wilson, N. Sutin, *J. Am. Chem. Soc.* **1977**, *99*, 3886.
36 Y. Ohgo, S. Neya, T. Ikeue, M. Takahashi, M. Takeda, N. Funasaki, M. Nakamura, *Inorg. Chem.* **2002**, *41*, 4627.
37 K. Rachlewicz, L. Latos-Grażyński, E. Vogel, Z. Ciunik, L. B. Jerzykiewicz, *Inorg. Chem.* **2002**, *41*, 1979.
38 G. A. Caignan, R. Dushmukh, Y. Zeng, A. Wilks, R. A. Bunce, M. Rivera, *J. Am. Chem. Soc.* **2003**, *125*, 11842.